doi.org/10.36721/PJPS.2023.36.6.SP.1891-1899.1

Guizhi longgu muli decoction ameliorates pathological changes in heart and bone in ovariectomized rats

Yuhan Wang, Pei Li, Jing Hu, Ying Yang, Qiqi Yan, Haixia Liu, Yanjing Chen* and Zhiguo Zhang*
Institute of Basic Theory, China Academy of Chinese Medical Sciences, Beijing, PR China

Abstract: The aim of this study is to investigate the pathological changes in cardiac function, blood pressure, blood lipids and bone metabolism in ovariectomized (OVX) rats, as well as the intervention effect of Guizhi Longgu Muli decoction (GZLM). Bilateral oophorectomy was used to establish an OVX menopausal model. Four groups of rats were randomly selected: Sham surgery group, OVX group, estradiol (0.018g/L) and GZLM group (20g/kg). Cardiac function was assessed using ultrasound, blood pressure was measured using the tail cuff method. The oxidase method was used to determine the total cholesterol (TC) and triglycerides in serum. Direct measurement of high-density lipoprotein and low-density lipoprotein levels (LDL-C). Hematoxylin eosin staining and electron microscopy examination of myocardial structure. Microscopic CT was used to determine the bone microstructure. GZLM improved pathological cardiac changes and reduced the LVIDs, LVVols and LVVold. There was a decrease in systolic pressure, diastolic pressure and mean blood pressure in GZLM group. A decrease in serum TC and LDL-C levels was observed in the GZLM group. The BMD, BV/TV, Tb.Th, Tb.N of GZLM group raised, while Tb.SP and SMI significantly decreased or decreased. GZLM may have the effect of improving abnormal cardiac structure and function, promoting bone metabolism in OVX rats.

Keywords: Guizhi longgu muli decoction, ovariectomized rats, cardiac function, bone metabolism.

INTRODUCTION

Most women experience menopausal symptoms, which may be severe and long-lasting in many cases. Most women experience vascular symptoms during the transitional period of menopause (over 80%), including hot flashes and night sweats. Women may also experience different prevalent symptoms with sleep disorders, fatigue, low mood and increased anxiety included (Talaulikar 2022). However, menopausal symptoms are often heterogeneous and if remain untreated, they may result in dissimilar severe diseases, like cardiovascular disease (CVD), hypertension and osteoporosis (Kang *et al.,* 2023).

The most prevalent reason of death worldwide is cardiovascular disease, accounting for 31% of all deaths (Wang *et al.,* 2022). Additionally, the burden of cardiovascular disease on society is enormous. It accounts for a large proportion of global healthcare expenditures and damages productivity (Evans *et al.,* 2020). It should be noted that cardiovascular disease in women is greatly influenced by menopause (Nappi *et al.,* 2022). Some studies suggest this is mainly attributed to sex hormones such as estrogen and its receptors (Nappi *et al.,* 2022). It is now understood that women who are exposed to endogenous estrogen during reproductive years are protected against cardiovascular disease, which disappears approximately 10 years after menopause (Regitz-Zagrosek Seeland 2011). Postmenopausal women are more likely to experience cardiac dysfunction and women are more likely to suffer from heart failure (HF) (Regitz-Zagrosek Seeland 2011). Much emphasis should be placed on HF with preserved ejection fraction (HFpEF), as it is more prevalent among women and accounts for nearly half of all hospitalizations due to HF (Kurrelmeyer 2017). Although the mortality rate of HFpEF patients is slightly higher, the readmission rate is comparable to that of HF patients with reduced ejection fraction (HFrEF) (Kurrelmeyer 2017). However, the cardiac function of menopausal model rats has been largely understudied, emphasizing the need for more research on changes in cardiac function in OVX rats.

Hypertension is a major cardiovascular risk factor affecting 25% of women, and its burden on women is greater than that on men (Wenger *et al.,* 2018; Zilberman 2018). There is a strong correlation between it and death, cardiovascular disease, and other diseases (Wenger *et al.,* 2018; Zilberman 2018). It is more likely that women who suffer from hypertension will experience adverse pathophysiological consequences compared to men, like left ventricular hypertrophy, increased arterial stiffness, diabetes, etc (Wenger *et al.,* 2018). Meanwhile, the primary risk factor for HFpEF and the largest single cause of cardiovascular death in the United States is hypertension (Kurrelmeyer 2017). Current evidence suggests that postmenopausal hormone changes and hypertension may lead to higher levels of target organ damage and cardiovascular diseases with increased arteriosclerosis, coronary heart disease, chronic HF and stroke included (Zilberman 2018).

*Corresponding author: e-mail: zzgtcm@163.com; chenyj010@163.com #Equally contributed

An abnormal blood lipid profile, increased fat content, and insulin resistance are associated with the menopause transition (Nappi *et al.,* 2022). In this respect, menopause is characterized by changes in circulating lipid levels in the blood with low-density lipoprotein (LDL-C), high-density lipoprotein (HDL-C) and triacylglycerol (TG) included (Ko Kim 2020). It should be emphasized that menopause increases blood LDL-C levels and CVD risk (Thaung Zaw *et al.,* 2018). Animal experiments have shown that in women who undergo oophorectomy or who consume E2 after menopause, the expression of genes that are required for effective energy consumption may be decreased, as well as postmenopausal women may be at risk of obesity and metabolic disorders due to genes involved in fat metabolism and lipid catabolism (Al-Safi Polotsky 2015). Whereas the basic and clinical research do not come to the same conclusion. According to research targeting 350 women in the perimenopausal stage, over 50% had HDL-C abnormalities, while 40% had high TG levels (Sharma *et al.,* 2016). Compared with premenopausal women, postmenopausal women have elevated levels of TG and TC (Sharma *et al.,* 2016). A meta-analysis also pointed out that postmenopausal women had significantly higher TG, TC and LDL-C levels than premenopausal women, while there was no significant difference in HDL-C levels among premenopausal women (Ambikairajah *et al.,* 2019). An investigation of the blood lipid levels of Chinese women in perimenopause and postmenopause indicated that women postmenopausal had higher levels of TC, TG and LDL-C than women in perimenopause, while the HDL-C's levels were lower (Cui *et al.,* 2016).

While both men and women typically reach peak bone mass around the age of 28 to 30 years, certain postmenopausal women experience accelerated bone loss by virtue of reduced estrogen levels. Bone loss may begin during perimenopause and result in a decrease in bone density by 2.5% annually (Lobo Gompel 2022). During menopause, estrogen deficiency causes bones to lose density and osteoclast activity increases rather than osteoblasts (Tella Gallagher 2014). Therefore, it is worth studying the bone metabolism of menopausal model rats that simulate menopausal women.

In addition to preventing osteoporosis, estrogens, particularly estrogen type 2, protect the cardiovascular system (Ko Kim 2020), especially in women at high risk of fractures (Kang *et al.,* 2023). However, estrogen therapy (ET) has many side effects and contraindications (Takahashi Johnson 2015). Common side effects include breast tenderness and vaginal bleeding and its contraindications include a history of coronary artery disease or stroke, hypertension, etc. (Takahashi Johnson 2015). As early as 2002, the Women's Health Initiative indicated that the overall harm of estrogen to disease prevention outweighed its benefits (Takahashi Johnson 2015). Although ET and estrogen and progesterone therapy reduce the risk of osteoporosis, they are related to the increased risk of stroke, venous thrombosis, gallbladder disease and incontinence (Takahashi Johnson 2015). Similarly, some drugs currently approved for the treatment of osteoporosis have many complications related to their use, which limits patients' acceptance of osteoporosis therapy (Khosla Shane 2016).

Traditional Chinese medicine formulas have yielded promising effects in treating various menopausal symptoms. Current evidence suggests that Guizhi Longgu Muli decoction (GZLM), a traditional Chinese medicine prescription, yields a favorable intervention effect on perimenopausal tachyarrhythmia and heart rate variability, serum E_2, follicle-stimulating hormone, etc. (Wang *et al.,* 2023). There is ample evidence that GZLM and its modified prescriptions have good effects in treating hypertension with insomnia (Meng Hongbai 2021; Mu 2021). In addition, there are reports on treating perimenopausal syndrome using this decoction (Ma *et al.,* 2020). Therefore, we speculate that it has a good intervention effect on various menopausal symptoms and can improve the cardiovascular system and bone metabolism in menopausal women. The purpose of this research was to investigate the effects of GZLM on menopausal women's cardiovascular system and bone metabolism through animal experiments and provide potential treatment methods for menopausal women.

MATERIALS AND METHODS

Animal models and preparation of herbs

In this study, we used 32 SPF grade female Sprague Dawley rats (average weight 230±15g; 10 weeks old). The animals were housed in a clean animal room at the Laboratory Animal Center of the Institute of Basic Theory for Chinese Medicine, China Academy of Chinese Medical Sciences. The temperature of the animal room is (24±2°C). The humidity is (45-60%) and the diurnal cycle time is 12:12 hours. Food and water are provided at will. This plan is authorized by the Institutional Ethics Committee of the China Academy of Chinese Medical Sciences (Approval Number: IBTCMCACMS2-1109-07). A week after adapting to the new diet, anesthesia was administered intraperitoneally with 3% pentobarbital sodium to 24 female SD rats at random (0.13mL/100 g). After preparing the skin, the abdomen was disinfected with iodine solution. Two incisions of about 1cm were made at the junction of 1 cm below the rib margin and 1 cm on both sides of the spine. Muscles and peritoneum were separated in sequence, and cauliflower-like ovaries were ligated in the abdominal fat and bilateral ovaries were removed. The tissue was then placed back into the abdominal cavity of the rats, Layer by layer stitching. The sham surgery group consisted of 8 rats who underwent ovarian resection to remove small adipose tissue in the abdominal cavity without removing the ovaries. After surgery, penicillin was injected intraperitoneally to

prevent infection. One week after surgery, a vaginal smear examination was performed once a day for 5 consecutive days to determine whether the estrous cycle had disappeared based on the morphology of vaginal smear cells. Successful modeling was observed when rats did not exhibit an estrous cycle.

To prepare GZLM, the following ingredients were used: Cinnamomum cassia Presl (9g), Paeoniae Radix Alba (9 g), Zingiberis Rhizoma (9g), *Ziziphus jujuba* Mill. (9g), Os Draconis (24g), Ostreae Concha (24g), Glycyrrhizae Radix et Rhizoma (6g). The first decoction was boiled in water with a volume of 10 times the mass of the medicinal material and then changed to low heat for 1 hour. The second decoction was boiled in water with a volume of 8 times the mass of the medicinal material, using the same method as the first decoction. The second decoction was mixed, concentrated to 2g (raw medicine)/ mL, and stored in a refrigerator at 4°C.

Animal grouping and treatment

The 24 rats that successfully modeled were randomly divided into three groups: model group (OVX), estrogen group (E_2), and GZLM group (GZLM), and administration began 10 days after surgery. In the E_2 group, we prepared a solution containing 0.018g/L of estradiol valerate tablets dissolved in 500mL of physiological saline. This solution was administered orally via gavage at a dose of 1.8×10^{-4}g/ kg. In the GZLM group, the rats were administered a dosage of 20g/ kg of the GZLM preparation once a day. This experiment is our first animal experiment using GZLM, and 20g/kg is our first dose given to rats. The use of this dose was determined based on our comprehensive literature review (Fu B 2020; Zhao Y 2019). This dose is two times the equivalent dose conversion between rats and humans. The commonly used dosage in clinical practice is 1-2 times the dosage of this formula, so we chose a dosage of 2 times for our study. Both the E_2 and GZLM treatments were given daily for 12 consecutive weeks, with a 6-day break between each week. Following the same method as the treated groups, equal volumes of distilled water were gavaged to the SHAM group and OVX group.

Indicator detection

General state observation, weight weighing and organ index measurement

Assessment of cardiac structure and function

During the 12 weeks treatment period, rats fasted for 12 hours before undergoing echocardiography (UCG) to measure cardiac function and structure. The rats' chests were prepared by applying depilatory cream for skin preparation, followed by applying a coupling agent. To ensure anesthesia, the rats continuously inhaled a mixture of isoflurane and pure oxygen, maintaining their heart rate at approximately 350 beats per minute. An operating table was set up with the rat in the supine position. And we used a 21Hz probe to take a short axis section of the rat's left ventricle and the M-type UCG sampling line sampled at the papillary muscle level. During the echocardiography procedure, a minimum of 10 cardiac cycles were continuously recorded. From these recordings, measurements and calculations were conducted on a variety of parameters, including short axis shortening rate (FS%), ejection fraction (EF%), left ventricular end-systolic diameter (LVIDs), left ventricular end-diastolic diameter (LVIDd), left ventricular posterior wall end-systolic thickness (LVPWs), left ventricular posterior wall end-diastolic thickness (LVPWd), left ventricular end-systolic volume (LVVols), and left ventricular end-diastolic volume (LVVold). All measured values are taken as the average of 3 cardiac cycles.

BP measurement

After 12 weeks of administration, each group of rats was measured for SBP, DBP and MBP in the tails of each animal, and heart rate using the BP-98A non-invasive BP collection system using the tail-cuff method. During the experiment, the insulation tube was kept at 38 degrees Celsius and the rats were acclimated to a dark experimental environment in advance. In order to determine their blood pressure and heart rate, we measured the rats after their condition stabilized. Three measurements were taken continuously from each rat, and the average was taken for each data point. The BP-98A non-invasive blood pressure collection system was used to collect data.

Detection of blood biochemical indicators

Using the Olympus fully automated biochemical analyzer AU480, the serum levels of TC and TG were detected using the oxidase method, and the serum levels of LDL-C and HDL-C were detected using the direct method.

HE staining and electron microscopy

After 12 weeks of treatment, fresh rat hearts were taken, rinsed with ice physiological saline, and the ventricles were transected and immediately fixed in a 4% paraformaldehyde solution. The hearts were stored at 4°C for testing. Additionally, a longitudinal section of the rat's left ventricle, measuring approximately 1 mm × 1 mm × 1 mm, was taken. This section was immediately fixed in a 4% glutaraldehyde solution and stored at 4°C for testing purposes. Standard techniques were employed, including embedding and fixing the myocardial tissue, performing HE staining, slicing the samples and conducting observations. Furthermore, transmission electron microscopy was applied to explore the ultrastructure of myocardial tissue.

Micro-CT detection of bone tissue

Micro-CT was performed using the Bruker Skyscan instrument 1276 micro-CT system (v1.6) (USA). The rat femur was scanned with a scanning resolution of 10.2μm and a field of view of 2016*1344 at a voltage of 70 kV and a current of 200μA. Taking the lowest point of the

lateral growth plate of the femoral knee as the baseline, the area with a thickness of 3mm was set as the 3D reconstruction area of interest. N-Recon software was used for 3D image reconstruction, and CT-AN software for bone trabecular distribution and BMD analysis.

Ethical approval

The present study was approved by the Institutional Ethics Committee of the China Academy of Chinese Medical Sciences (approval No. IBTCMCACMS21-2109-07). Written informed consent was obtained from all participants.

STATISTICAL ANALYSIS

Statistical software SPSS 20.0 was applied to analyze the data, and the mean and standard deviation are presented as the results. Comparations between multiple groups were conducted using one-way ANOVA, and pairwise comparisons were conducted using the LSD test if the variance was homogeneous. The Kruskal-Wallis nonparametric test was used when the variance was not homogeneous, and the Bonferroni method was used for pairwise comparisons. Statistical significance was determined by a *P* value of 0.05.

RESULTS

Weight and organ index of OVX rats after administration of GZLM

As shown in fig. 1, body weight of OVX group rats was significantly higher than that of SHAM group rats (P<0.01). In comparison to the OVX group, neither the E_2 nor GZLM groups changed significantly in body weight. Moreover, there was no significant difference in cardiac index among the groups of rats. As compared with the SHAM group, rats in the OVX group had a significantly lower uterine coefficient (P<0.01). Neither the E_2 nor GZLM groups had significantly different uterine coefficient from the OVX group.

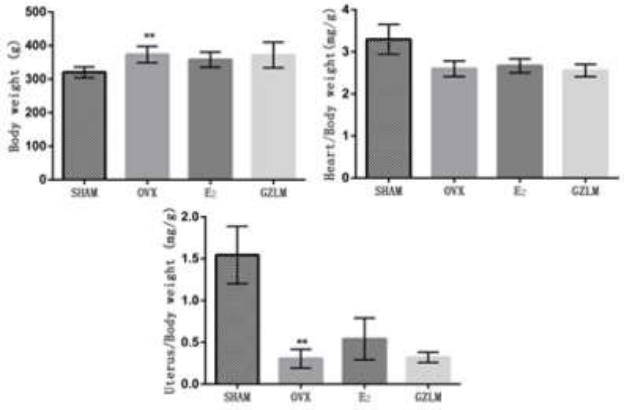

Fig. 1: GZLM effects on body mass and organ coefficient in OVX rats.

Compared with the SHAM group, *p<0.05, **p<0.01; Compared with the OVX group, $^{\triangle}p$<0.05, $^{\triangle\triangle}p$<0.01.

The effect of GZLM on cardiac function in ovariectomized rats

LVIDs, LVVols, LVIDd and LVVold were significantly higher in the OVX group compared with the SHAM group (P<0.01). Although EF% and FS% exhibited a downward trend, there was no significant difference. There was a decrease in LVVols in the E_2 group, compared to the OVX group (P<0.05). Moreover, the LVIDs, LVVols and LVVold in the GZLM group reduced (P<0.05) (fig. 2).

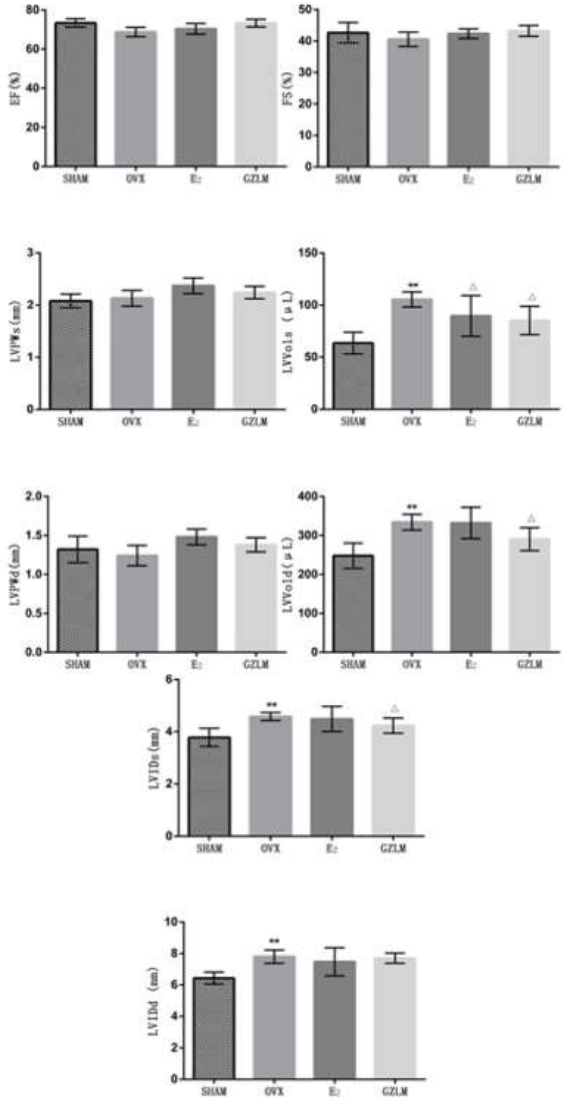

Fig. 2: Cardiovascular function of OVX rats treated with GZLM.

Compared with the SHAM group, *p<0.05, **p<0.01; Compared with the OVX group, $^{\triangle}p$<0.05, $^{\triangle\triangle}p$<0.01.

Ovariectomy-induced changes in blood pressure and heart rate in rats treated with GZLM

A significant increase in SBP was observed in rats treated with OVX in comparison to the SHAM group (P<0.01).

Moreover, rats in the E_2 group exhibited significantly reduced SBP, DBP and MBP (P<0.01) contrasted with the OVX group. GZLM rats had significantly decreased SBP, DBP and MBP (P<0.05 or P<0.01), while heart rates were not significantly different between groups (fig. 3).

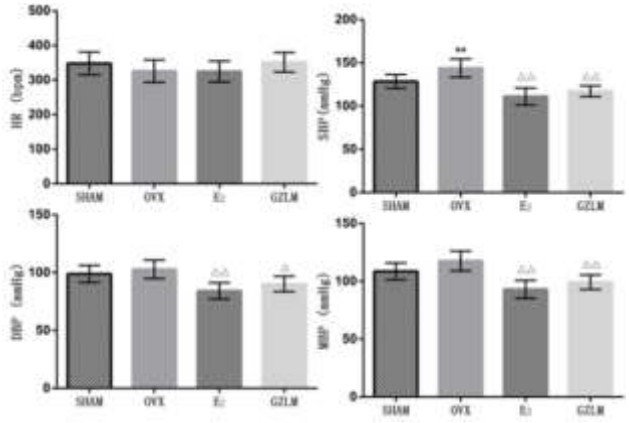

Fig. 3: The effect of GZLM on BP and heart rate in OVX rats.
Compared with the SHAM group, *p<0.05, **p<0.01; Compared with the OVX group, $^{\triangle}p$<0.05, $^{\triangle\triangle}p$<0.01.

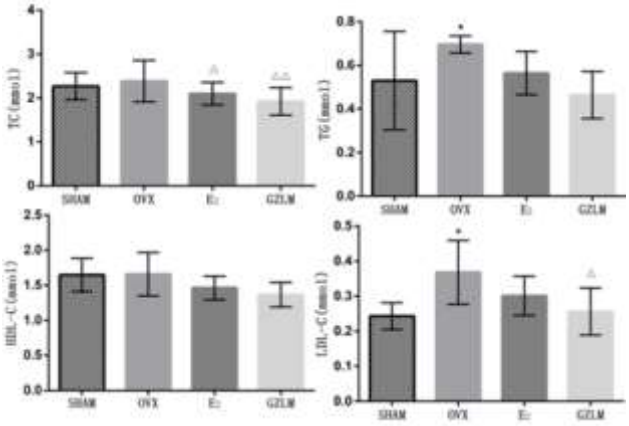

Fig. 4: GZLM's effects on blood lipids in OVX rats.
Compared with the SHAM group, *p<0.05, **p<0.01; Compared with the OVX group, $^{\triangle}p$<0.05, $^{\triangle\triangle}p$<0.01.

GZLM affects blood lipids in ovariectomized rats

In comparison to the SHAM group, serum TG and LDL-C levels in OVX rats increased (P<0.05). A decrease in serum TC level was observed in the E2 group in comparison to the OVX group (P<0.05). Moreover, there was a significant decrease in serum TC and LDL-C levels in rats of the GZLM group (P<0.05 or P<0.01) (fig. 4).

Effect of GZLM on myocardial HE and electron microscopic pathological changes in OVX rats

Upon completion of 12 weeks of treatment, examination of myocardial histology by HE staining and transmission electron microscopy revealed that the myocardial stripes in the SHAM group exhibited a well-organized and dense arrangement, with orderly aligned myocardial cells and clear sarcomere structure. SHAM group myocardial mitochondria had intact membranes and clearly defined cristae. Myocardial fibers in the OVX group were atrophying and thinning and there was an increase in the gap between the cells of the heart. The ultrastructural analysis of the myocardium showed that the myocardial myofibril arrangement was disordered, myofilaments were irregular and the myocardial mitochondrial crista was significantly broken and sparse. The myocardial stripes of the E_2 group rats were obvious, with occasional myocardial cell atrophy, focal interstitial hyperplasia, neatly arranged myofilaments and a well-defined mitochondrial ridge structure.

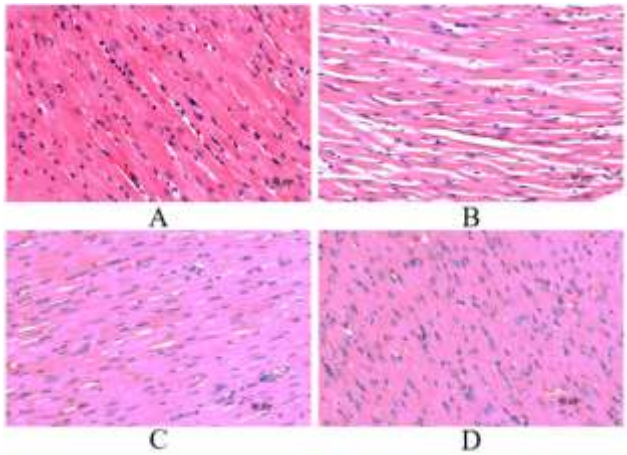

Fig. 5: The effect of GZLM on the myocardium of OVX rats (HE staining, ×200). A. SHAM B. OVX C. E_2 D. GZLM

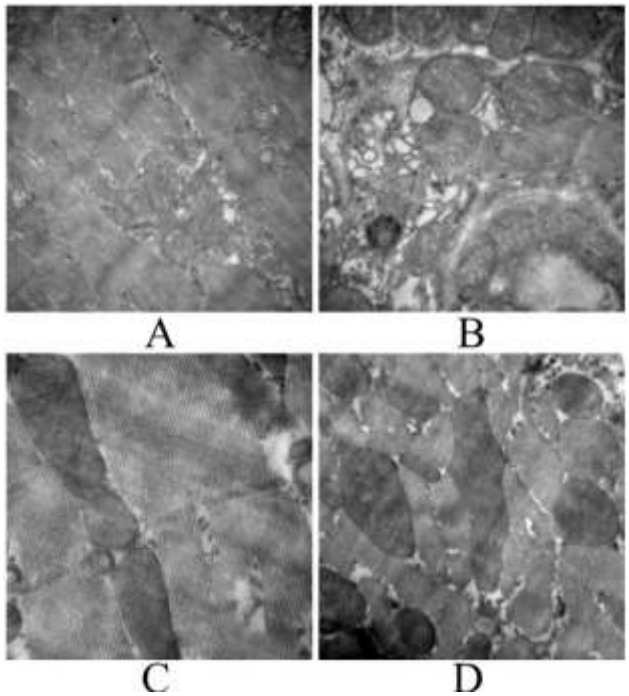

Fig. 6: The Effect of GZLM on the Ultrastructure of Myocardium in OVX Rats (electron microscopy staining, ×30000). A. SHAM B. OVX C. E_2 D. GZLM

Myocardial cell atrophy and matrix hyperplasia in the GZLM group were milder than in the OVX group, with intact mitochondrial membranes and well-defined mitochondrial ridge structures. According to the above outcomes, the pathological changes in myocardial structure of OVX rats could be improved by both E_2 and GZLM (figs. 5 and 6).

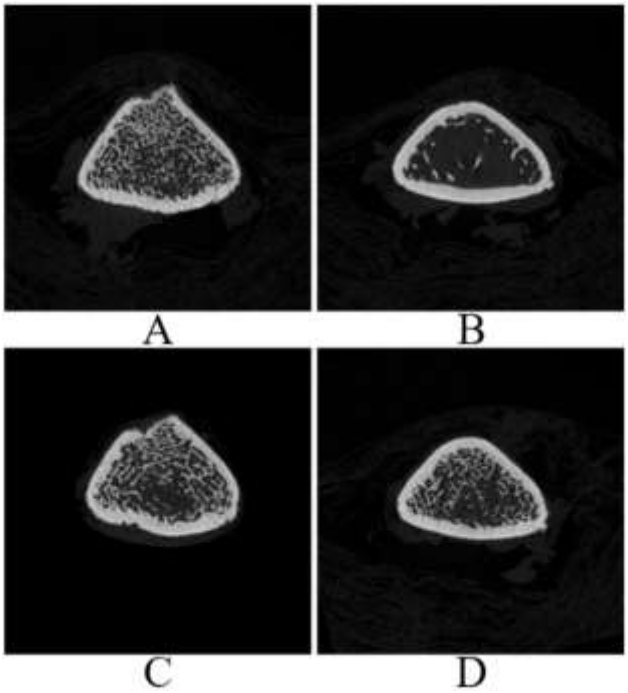

Fig. 7(a): The effect of GZLM on the tissue structure of the femur in OVX rats.
A. SHAM B. OVX C. E_2 D. GZLM

Bone trabecular microstructure

After 12 weeks of treatment, in comparison to the SHAM group, the microstructure of the femoral tissue in the OVX group was impaired, with sparse bone trabeculae and interrupted connections. Compared with the OVX group, the bone trabecular structure in the E_2 and GZLM groups was relatively intact and bone tissue damage was less severe. Fig. 7(a) illustrates the above pathological findings.

As shown in fig. 7(b), in contrast to the SHAM group, the BMD, BV/TV, Tb.N of OVX rats were significantly reduced (P<0.01), whereas Tb.SP and SMI were raised (P<0.01). The E2 and GZLM groups showed significant increases in BMD, BV/TV, Tb.Th and Tb.N (P<0.05 or P<0.01), while the OVX group showed significant decreases in Tb. SP and SMI (P<0.05 or P<0.01).

DISCUSSION

The decrease in estrogen production in the ovaries during menopause can lead to symptoms of physical weakness, including metabolic changes in susceptibility to cardiovascular disease and hyperlipidemia, as well as bone loss (da Silva *et al.,* 2022). Although E_2 yields protective effects on the cardiovascular and skeletal systems, its side effects cannot be underestimated (Kang *et al.,* 2023; Ko Kim 2020; Takahashi Johnson 2015). There is an increasing consensus that traditional Chinese medicine formulas yield a significant regulatory effect on menopausal women. In this respect, GZLM decoction has been demonstrated to improve female menopausal symptoms (Ma *et al.,* 2020; Wang *et al.,* 2023).

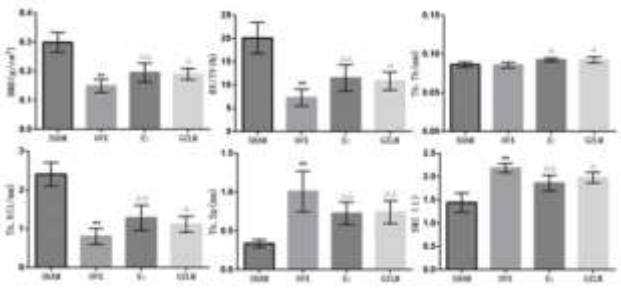

Fig. 7(b): The effect of GZLM on the structural parameters of bone trabeculae in OVX rats.
Compared with the SHAM group, *p<0.05, **p<0.01; Compared with the OVX group, $^{\triangle}p$<0.05, $^{\triangle\triangle}p$<0.01.

In an experimental study, the OVX rats' body weight significantly raised, and the uterine coefficient significantly decreased (Davis *et al.,* 2015). There is literature indicating that rats treated with estradiol injection have higher body weight than the normal control group. The results of this experiment are similar (Diaz *et al.,* 2023). Consistently, OVX group participants showed a significant increase in body weight and a significant decrease in uterine coefficient in the present study. Whereas there was no significant change in body weight in the GZLM groups. Additionally, different groups did not have significantly different heart coefficients.

It is now understood that the incidence of diastolic dysfunction is higher in postmenopausal women (Mori *et al.,* 2011). Mori T et al.'s study showed that ovariectomy and constriction of the renal aorta could increase left ventricular end-diastolic pressure in rats. Importantly, β-estradiol replacement could prevent diastolic dysfunction in model rats (Mori *et al.,* 2011). In a study by Bustamante et al., the cardiac chamber diameter in the OVX group significantly increased over time, while EF and FS showed no significant abnormal changes (Bustamante *et al.,* 2019). The decrease in E_2 further exacerbated this change, resulting in a significant decrease in cardiac output while maintaining normal EF (Barton Meyer 2009). In the present study, LVIDs, LVVOls, LVIDd, and LVVOld of OVX rats remarkably increased, while EF and FS only slightly decreased. GZLM decreased the above indicators, respectively. This finding indicated that the systolic and diastolic functions of OVX rats were abnormal, and GZLM improved the cardiac function of OVX rats.

Elevated BP is a common pathological change in menopausal women, with over 70% of postmenopausal women (aged over 60 years) in the United States suffering from hypertension (Barton Meyer 2009). Women postmenopausal are more likely to experience hypertension than men their age and hypertension is more common in women than in men. There are reports that a 10mmHg increase in SBP increases CVD risk in women by 25%, while it increases risk in men only by 15% (Wei *et al.,* 2017). According to the current research, the OVX rats' BP increased, primarily in SBP, with some increases in diastolic and mean blood pressure, but no significant difference was found (Li *et al.,* 2020). However, the SBP, DBP, and MBP of the GZLM groups decreased, suggesting that GZLM has a good antihypertensive effect. Elevated blood pressure may lead to myocardial hypertrophy. However, in this experiment, although the blood pressure of OVX rats increased, according to their cardiac HE pathological results, their left ventricle did not show hypertrophy, but showed focal atrophy, similar to previous studies (Wang *et al.,* 2022). This is worth further research.

As a result of menopause, body fat can increase and redistribute (Davis *et al.,* 2015). In some cases, fat transfer from the periphery to the trunk results in a raise in visceral fat (Davis *et al.,* 2015). Abdominal obesity and decreased estrogen levels during menopause are closely related to bad reactions (Barton Meyer 2009; Tchernof Després 2013). Metabolic changes like insulin resistance have the tendency to advance into type 2 diabetes and symptoms of dyslipidemia include high triglycerides, decreased HDL cholesterol, and small and dense HDL particles (Barton Meyer 2009; Tchernof Després 2013). E_2 intervention can reduce LDL-C and TC in OVX rats, which may be related to its reduction in the activity of lipoprotein lipase (Azizian *et al.,* 2021). In addition, E_2 directly helps maintain insulin sensitivity in the early stages of metabolic dysfunction development, possibly by preventing low-grade inflammation in white adipose tissue (Shen *et al.,* 2014). In this experiment, the TG, LDL-C and TC levels increased, but no significant difference was observed. However, treatment with GZLM mitigated the raise in TC, TG and LDL-C levels in OVX rats.

The skeleton is a dynamic tissue, and the process of bone formation and bone absorption occurs continuously throughout an individual's life, maintaining a dynamic balance (Davis *et al.,* 2015). Current evidence suggests decreased estrogen after menopause leads to bone uncoupling and remodeling and excessive bone resorption (Davis *et al.,* 2015). More specifically, estrogen deficiency can lead to the cytokine RANKL (receptor nuclear factor) κ B ligand activator), which promotes osteoclast generation and bone resorption on the surface of its receptor RANK (also known as TNFRSF11A) pre-osteoclast and mature osteoclast (Boyle *et al.,* 2003). As a natural RANKL inhibitor, osteoprotectin (OPG) is secreted by osteoblasts in response to estrogen stimulation (Boyle *et al.,* 2003; Tella Gallagher 2014). Decreased OPG leads to increased RANKL activity in estrogen-deficient women (Boyle *et al.,* 2003; Tella Gallagher 2014). In addition, age-related decreased intestinal calcium absorption and vitamin D deficiency result in secondary hyperparathyroidism through the kidneys. Additionally, this accelerates bone resorption (Davis *et al.,* 2015). In addition, preliminary studies on mice and humans have shown that bone loss is caused by pro-inflammatory cytokines following estrogen withdrawal (Clowes *et al.,* 2005). E_2 can improve bone resorption markers, enhance bone formation markers, and inhibit inflammation (Azmy Abd El-Motelp B *et al.,* 2021). Other studies have shown that T and B lymphocytes mediate estrogen's effect on bone weight (Almeida *et al.,* 2017). The interaction between the gut micro biota and the immune system is concerned with the impact on the bone formation of OVX model mice (Lorenzo 2021). In this experiment, the bone trabecular structure of OVX group rats was damaged, bone density decreased, and bone structural parameters underwent abnormal changes. GZLM improved sparse bone trabeculae, increased bone density and improved bone trabecular structural parameters in OVX rats.

CONCLUSION

In summary, the OVX rats exhibited abnormal changes in systolic and diastolic functions, including increased blood pressure and lipid levels, reduced bone density, and disruption of bone trabecular structure. GZLM significantly improved the cardiac function, BP, blood lipids, and the OVX rats' bone metabolism and played a protective role in the cardiovascular and skeletal systems of OVX rats. Based on these findings, GZLM may be a viable option for preventing and treating cardiovascular and skeletal disorders in menopausal women.

AKCNOWLEDGEMENT

This work was supported by the CACMS Innovation Fund (grant number CI2021A00107), the National Natural Science Foundation of China (Grant No. 82074297) and the Fundamental Research Funds for the Central Public Welfare Research Institutes (Grant Nos. YZ-202241, YZ-202244).

REFERENCES

Almeida M, Laurent MR, Dubois V, Claessens F, O'Brien CA, Bouillon R, Vanderschueren D and Manolagas SC (2017). Estrogens and androgens in skeletal physiology and pathophysiology. *Physiol. Rev.,* **97**(1): 135-187.

Al-Safi ZA and Polotsky AJ (2015). Obesity and menopause. *Best Pract. Res. Clin. Obstet. Gynaecol.,*

29(4): 548-553.

Ambikairajah A, Walsh E and Cherbuin N (2019). Lipid profile differences during menopause: A review with meta-analysis. *Menopause,* **26**(11): 1327-1333.

Azizian H, Khaksari M, Asadikaram G, Esmailidehaj M and Shahrokhi N (2021). Progesterone eliminates 17β-estradiol-mediated cardioprotection against diabetic cardiovascular dysfunction in ovariectomized rats. *Biomed. J*., **44**(4): 461-470.

Azmy Abd El-Motelp B, Tarek Ebrahim M and Khairy Mohamed H (2021). *Salvia officinalis* extract and 17β-estradiol suppresses ovariectomy induced osteoporosis in female rats. *Pak. J. Biol. Sci.,* **24**(3): 434-444.

Barton M and Meyer MR (2009). Postmenopausal hypertension: Mechanisms and therapy. *Hypertension,* **54**(1): 11-18.

Boyle WJ, Simonet WS and Lacey DL (2003). Osteoclast differentiation and activation. *Nature,* **423**(6937): 337-342.

Bustamante M, Garate-Carrillo A, B RI, Garcia R, Carson N, Ceballos G, Ramirez-Sanchez I, Omens J and Villarreal F (2019). Unmasking of oestrogen-dependent changes in left ventricular structure and function in aged female rats: A potential model for pre-heart failure with preserved ejection fraction. *J. Physiol.,* **597**(7): 1805-1817.

Clowes JA, Riggs BL and Khosla S (2005). The role of the immune system in the pathophysiology of osteoporosis. *Immunol. Rev.,* **208**(6): 207-227.

Cui Y, Ruan X, Jin J, Jin F, Brucker S and Mueck AO (2016). The pattern of lipids and lipoproteins during the menopausal transition in Chinese women. *Climacteric,* **19**(3): 292-298.

Da Silva FB, Romero WG, Rouver WDN, Silva K, de Almeida SA, Mengal V, Peluso AA, Endlich PW, Bissoli NS, Claudio ERG and de Abreu GR (2022). Ellagic Acid prevents vascular dysfunction in small mesenteric arteries of ovariectomized hypertensive rats. *J. Nutr. Biochem.,* **105**(30): 108995.

Davis SR, Lambrinoudaki I, Lumsden M, Mishra GD, Pal L, Rees M, Santoro N and Simoncini T (2015). Menopause. *Nat. Rev. Dis. Primers.,* **1**(23): 15004.

Diaz JC, Dunaway K, Zuniga C, Sheil E, Sadeghian K, Auger AP and Baldo BA (2023). Delayed estrogen actions diminish food consumption without changing food approach, motor activity, or hypothalamic activation elicited by corticostriatal μ-opioid signaling. *Neuropsychopharmacol.,* **48**(13): 1952-1962.

Evans MA, Sano S and Walsh K (2020). Cardiovascular disease, aging, and clonal hematopoiesis. *Annu. Rev. Pathol.,* **15**(1): 419-438.

Fu B (2020). Effects of *Guizhi jialonggu oyster* soup on blood lipids and hcy in rats with autonomic nervous function impairment and carotid atherosclerosis [D]. University of Shandong Traditional Chinese Medicine, pp.2-19.

Kang HG, Kim HY, Jee H, Jun H, Cho H, Park D, Ahn HJ, Kim HM and Jeong HJ (2023). Compound of *Cynanchum wilfordii* and *Humulus lupulus* L. ameliorates menopausal symptoms in ovariectomized mice. *Reprod. Sci.,* **30**(5): 1625-1636.

Khosla S and Shane E (2016). A crisis in the treatment of osteoporosis. *J. Bone. Miner. Res.,* **31**(8): 1485-1487.

Ko SH and Kim HS (2020). Menopause-associated lipid metabolic disorders and foods beneficial for postmenopausal women. *Nutrients,* **12**(1): 202-227.

Kurrelmeyer K (2017). Cardiovascular disease in women. *Methodist. Debakey Cardiovasc. J.,* **13**(4): 183-184.

Li Y, Zhang W, Li J, Sun Y, Yang Q, Wang S, Luo X, Wang W, Wang K, Bai W, Zhang H and Qin L (2020). The imbalance in the aortic ceramide/sphingosine-1-phosphate rheostat in ovariectomized rats and the preventive effect of estrogen. *Lipids. Health Dis.,* **19**(1): 95.

Lobo RA and Gompel A (2022). Management of menopause: A view towards prevention. *Lancet Diabetes Endocrinol.,* **10**(6): 457-470.

Lorenzo J (2021). From the gut to bone: Connecting the gut micro biota with Th17 T lymphocytes and postmenopausal osteoporosis. *J. Clin. Invest.,* **131**(5): e146619.

Ma T, Li J, Zhang Y, Gu C and Zhang Y (2020). Clinical application of Guizhi Jia Longgumuli Tang. *J. Gansu Univer. Chin. Med.,* **37**(02): 92-95.

Meng L and Hongbai Q (2021). Curative effect of Guizhi plus *Longgu oyster* soup on hypertension with insomnia. *Chin. J. Mod. Drug Appl.,* **15**(14): 208-210.

Mori T, Kai H, Kajimoto H, Koga M, Kudo H, Takayama N, Yasuoka S, Anegawa T, Kai M and Imaizumi T (2011). Enhanced cardiac inflammation and fibrosis in ovariectomized hypertensive rats: A possible mechanism of diastolic dysfunction in postmenopausal women. *Hypertens. Res.,* **34**(4): 496-502.

Mu J (2021). Clinical effect of Guizhi plus *Longgu oyster* soup on hypertension with insomnia. *Cardiovascular Disease Electronic J. Integrated Tra. Chin. West. Med.,* **9**(09): 61-63.

Nappi RE, Chedraui P, Lambrinoudaki I and Simoncini T (2022). Menopause: A cardiometabolic transition. *Lancet Diabetes Endocrinol.,* **10**(6): 442-456.

Regitz-Zagrosek V and Seeland U (2011). Sex and gender differences in myocardial hypertrophy and heart failure. *Wien. Med. Wochenschr.,* **161**(5-6): 109-116.

Sharma S, Aggarwal N, Joshi B, Suri V and Badada S (2016). Prevalence of metabolic syndrome in pre- and post-menopausal women: A prospective study from apex institute of North India. *J. Midlife. Health,* **7**(4): 169-174.

Shen M, Kumar SP and Shi H (2014). Estradiol regulates insulin signaling and inflammation in adipose tissue. *Horm. Mol. Biol. Clin. Investig*., **17**(2): 99-107.

Takahashi TA and Johnson KM (2015). Menopause. *Med. Clin. North Am.,* **99**(3): 521-534.

Talaulikar V (2022). Menopause transition: Physiology

and symptoms. *Best Pract. Res. Clin. Obstet. Gynaecol.*, **81**(03): 3-7.

Tchernof A and Després JP(2013). Pathophysiology of human visceral obesity: An update. *Physiol Rev.*, **93**(1): 359-404.

Tella SH and Gallagher JC (2014). Prevention and treatment of postmenopausal osteoporosis. *J. Steroid. Biochem. Mol. Biol.*, **142**(09): 155-170.

Thaung Zaw JJ, Howe PRC and Wong RHX (2018). Postmenopausal health interventions: Time to move on from the Women's Health Initiative? *Ageing Res. Rev.*, **48**: 79-86.

Wang Y, Jiang Y, Hu J, Yang Y, Liu Y, Liu H, Zhang Z and Chen Y (2022). Dynamic evolution of cardiac function and glucose and lipid metabolism in ovariectomized rats and the intervention effect of erxian decoction. *Evid. Based Complement. Alternat. Med.*, **17**: 8090868.

Wang Y, Wang X and Gao W (2023). Effect of Guizhi plus Longgu oyster decoction on perimenopausal tachyarrhythmia and HRV, E2, FSH [J]. Journal of Liaoning University of Traditional Chinese Medicine, *J. Liaoning Univer.Tra. Chin. Med.*, **25**(03): 10-13.

Wei YC, George NI, Chang CW and Hicks KA (2017). Assessing sex differences in the risk of cardiovascular disease and mortality per increment in systolic blood pressure: A systematic review and meta-analysis of follow-up studies in the united states. *PLoS One*, **12**(1): e0170218.

Wenger NK, Arnold A, Bairey Merz CN, Cooper-DeHoff RM, Ferdinand KC, Fleg JL, Gulati M, Isiadinso I, Itchhaporia D, Light-McGroary K, Lindley KJ, Mieres JH, Rosser ML, Saade GR, Walsh MN and Pepine CJ (2018). Hypertension across a woman's life cycle. *J. Am. Coll. Cardiol.*, **71**(16): 1797-1813.

Zhao Y (2019). Clinical examples of cinnamon twig and dragon bone Oyster decoction. *China's Naturopathy*., **27**(13): 94-96.

Zilberman JM (2018). Menopause: Hypertension and vascular disease. *Hipertens. Riesgo. Vasc.*, **35**(2): 77-83.